Title

Maximizing MR signal for 2D UTE slice selection in the presence of rapid transverse relaxation

Journal

Magnetic Resonance Imaging, 32(8)

ISSN

0730-725X

Authors

Carl, Michael
Chiang, Jing-Tzyh Alan
Du, Jiang

Publication Date

2014-10-01

DOI

10.1016/j.mri.2014.05.001

Published in final edited form as:
Magn Reson Imaging. 2014 October ; 32(8): 1006–1011. doi:10.1016/j.mri.2014.05.001.

Maximizing MR Signal for 2D UTE Slice Selection in the Presence of Rapid Transverse Relaxation

Michael Carl[1], **Jing-Tzyh Alan Chiang**[2], and **Jiang Du**[3]

[1]GE Healthcare, University of California, San Francisco

[2]Radiology Department, University of California, San Francisco

[3]Radiology Department, University of California, San Diego

Abstract

Ultrashort TE (UTE) sequences allow direct visualization of tissues with very short T2 relaxation times, such as tendons, ligaments, menisci, and cortical bone. In this work, theoretical calculations, simulations, and phantom studies, as well as in vivo imaging were performed to maximize signal-to-noise ratio (SNR) for slice selective RF excitation for 2D UTE sequences. The theoretical calculations and simulations were based on the Bloch equations, which lead to analytic expressions for the optimal RF pulse duration and amplitude to maximize magnetic resonance signal in the presence of rapid transverse relaxation. In steady state, it was found that the maximum signal amplitude was not obtained at the classical Ernst angle, but at an either lower or higher flip angle, depending on whether the RF pulse duration or amplitude was varied, respectively.

Keywords

RF Optimization; 2D UTE; Short T_2; Ernst Angle

Introduction

Clinical magnetic resonance (MR) imaging is predominantly geared towards visualizing relatively long T2 species, for which the radiofrequency (RF) pulse duration τ can be considered negligible compared to the intrinsic T2 of the tissues or fluids being studied. When using ultrashort TE (UTE) methods to image short or ultra short T2 species, such as ligaments, tendons or cortical bone, the intrinsic T2 can be on the same order as τ, and the signal decay during the RF pulse may become significant [1–6].

Author for Correspondence: Michael Carl, GE Healthcare, 408 Dickinson Street, San Diego, CA 92103-8226, (760) 855 7628 tele, (619) 471 0503 fax, Michael.carl@ge.com.

For two-dimensional (2D) UTE Robson et al [3] have shown significant effects of T2 decay on signal amplitude during shaped RF pulses. Springer et al [4] studied the effects of T2 decay during hard RF pulses relevant to three-dimensional (3D) UTE and concluded that the optimum flip angle for maximum signal for the case of constant RF pulse duration is always higher than the classical Ernst angle. Carl et al [5, 6] studied the case for constant RF pulse amplitude and concluded that the optimum flip angle for maximum signal in this situation is always lower than the classical Ernst angle, and derived analytic closed-form criteria (i.e. a "generalized Ernst angle") to maximize the available MR signal. Here this analysis is extended to slice selective shaped pulses used in 2D UTE (see Fig. 1) for RF pulses both of constant duration and constant amplitude.

Theory

The two parameters under the control of the pulse programmer that determine the nominal flip angle θ for a shaped RF pulse are the time dependent magnetic RF field strength $B_1(t)$ and pulse duration τ.

$$\theta = \gamma \int_0^{\tau} B_1(t)\, dt \quad (1)$$

Eq.[1] is only valid if one assumes $\tau \ll$ T2. Solving the Bloch equations in the small tip angle approximation (i.e. $\theta \ll \pi/2$) for the transverse magnetization M_T produced after a single RF pulse, using a slice selection gradient $G(t)$ in the presence of T2 relaxation leads to [7]:

$$M_T(\tau, z) = \gamma M_0 e^{-\frac{\tau}{T_2}} e^{-i\gamma z \int_0^{\tau} G(t)\, dt} \int_0^{\tau} B_1(t) e^{\frac{t}{T_2}} e^{i\gamma z \int_0^{t} G(t')\, dt'} dt \quad (2a)$$

The remaining longitudinal magnetization can be calculated by substituting the transverse magnetization (Eq.[2a]) back into the Bloch equation for the z-magnetization:

$$M_z(\tau, z) = M_0 - \gamma \int_0^{\tau} B_1(t) M_T(t, z)\, dt \quad (2b)$$

Through Bloch simulations it can be shown, that the whole available MR signal integrated over the region of the desired slice width is approximately proportional to the signal at the center of the slice. Hence, to a good approximation Eq.[2] can be evaluated at the center of the slice (z = 0), which simplifies the analysis. Solving Eq.[2] at z = 0 requires knowledge of $B_1(t)$, which with UTE sequences is usually VERSE (Variable-Rate Selective Excitation for Rapid MRI Sequence) corrected [8] and hence is not in a simple closed form. To obtain a solution, it is more straightforward to integrate Eq.[2] numerically as discrete sums using the actual discrete waveform profiles of $B_1(n)$ that are used when imaging (see Fig. 2).

The RF pulse profile is assumed to be a simple array of numbers containing N points, has a normalized raster time $\Delta t = 1$ μs corresponding to a duration of $\tau = N\Delta t$, and is normalized with maximum amplitude $B_1 = 1$ μT. The general RF duration τ and raster time Δt can be stretched by a factor α: ($\tau \rightarrow \alpha\tau$, $\Delta t \rightarrow \alpha\Delta t$) and the general RF amplitude can be changed

by an amplitude scaling factor β: $B_1 \rightarrow \beta B_1$. For example, a RF pulse file with N = 200 points, α = 4, and β = 5 would correspond to a raster time Δt = 4 μs, total duration of τ = 800 μs, and a maximum amplitude of B_1 = 5 μT. This allows investigation of the best pulse duration (i.e. the best stretch factor α), and/or the best amplitude scaling (i.e. the best amplitude scaling factor β) to maximize signal.

Spoiled RF pulse train

In clinical imaging the longitudinal magnetization is not usually allowed to re-grow to its equilibrium value M_0, so we now consider the case of a RF pulse train acquisition (θ→TR→θ→TR…). For a spoiled gradient recalled echo (SPGR) sequence, the steady state transverse magnetization M_{ss} (at z = 0) can be synthesized from M_T and M_z of Eq.[2], as explained in many standard textbooks e.g. [9] and is given by:

$$\begin{aligned} M_{SS}(\alpha\tau,\beta B_1) &= \frac{(1-E_1)}{1-E_1\frac{M_z}{M_0}} M_T \\ &= \alpha\beta(\gamma\Delta t M_0)(1-E_1)\frac{e^{-\frac{\alpha\tau}{T_2}}\sum_{n}^{N} B_1(n) e^{\frac{n\alpha\Delta t}{T_2}}}{1-E_1\left[1-(\alpha\beta\gamma\Delta t)^2\sum_{n}^{N}\sum_{j}^{n} B_1(n)B_1(j)e^{\frac{(j-n)\alpha\Delta t}{T_2}}\right]} \\ &\approx \frac{\alpha\beta e^{-\frac{\alpha\tau}{T_2}} f_0(\alpha)}{1-E_1+E_1(\alpha\beta\gamma\Delta t)^2 g_0(\alpha)} \end{aligned} \quad (3a)$$

where $E_1 \equiv \exp\left(-\frac{TR}{T_1}\right)$. The following definitions were used in the last step to simplify the equations:

$$\begin{aligned} f_0(\alpha) &\equiv \sum_{n=1}^{N} B_1(n) e^{\frac{n\alpha\Delta t}{T_2}} \\ g_0(\alpha) &\equiv \sum_{n=1}^{N}\sum_{j=1}^{n} B_1(n)B_1(j) e^{\frac{(j-n)\alpha\Delta t}{T_2}} \end{aligned} \quad (3b)$$

The expressions in Eq.[3b] can be easily calculated from the RF waveform file.

Maximizing MR signal

In order to maximize the steady state transverse magnetization, there are two basic approaches:

1. Keep τ fixed and optimize B_1, i.e. keep α fixed and optimize β.
2. Keep B_1 fixed and optimize τ, i.e. keep β fixed and optimize α.

Method 1) can be solved by setting the derivative of Eq.[3a] with respect to β equal to zero which yields:

$$\beta=\frac{1}{\gamma\alpha\Delta t}\sqrt{\frac{1-E_1}{E_1 g_0}}=\frac{1}{\gamma\alpha\Delta t}\sqrt{\frac{1-E_1}{E_1\sum_{n=1}^{N}\sum_{j=1}^{n}B_1(n)B_1(j)e^{\frac{(j-n)\alpha\Delta t}{T_2}}}} \quad (4)$$

This approach is mathematically simpler and is easier to implement, since the flip angle on clinical scanners can typically be changed by scaling the RF pulse amplitude of an externally loaded waveform while keeping its duration constant. On the other hand, the final calculated RF amplitude after optimization might be either higher than the hardware performance limit (and hence invalid) or significantly lower than the hardware performance limit, requiring iterative optimization to determine the best possible overall pulse. Finally, as was shown in Ref.[4] (and is reflected in Fig. 4a), when the RF duration is kept constant and the RF amplitude is varied the optimum flip angle for short T2 tissues is always greater than the classical Ernst angle $\theta_E=\cos^{-1}[\exp(-TR/T_1)]$ which does not take into account T2 effects during the RF pulse. This makes the optimum flip angle more likely to be positioned in a regime where the underlying small tip angle approximation (and hence Eq.[3a]) is no longer valid.

Method 2) can be solved by setting the derivative of Eq.[3a] with respect to α equal to zero which yields:

$$\begin{aligned}0=&\alpha^3\beta^2\gamma^2\Delta t^2E_1R_2\{\Delta t(f_1g_0-f_0g_1)-\tau f_0g_0\}-\alpha^2\beta^2\gamma^2\Delta t^2E_1f_0g_0\\&+\alpha R_2\{\tau f_0(E_1-1)+\Delta t\, f_1(1-E_1)\}+f_0(1-E_1)\end{aligned} \quad (5a)$$

The following additional definitions were used in the last step to simplify the equations:

$$\begin{aligned}f_1(\alpha)&\equiv\sum_{n=1}^{N}nB_1(n)e^{\frac{n\alpha\Delta t}{T_2}}\\g_1(\alpha)&\equiv\sum_{n=1}^{N}\sum_{j=1}^{n}(j-n)B_1(n)B_1(j)e^{\frac{(j-n)\alpha\Delta t}{T_2}}\end{aligned} \quad (5b)$$

Since Eq.[5a] is transcendental, it can only be solved numerically, which however is straightforward using the expressions in Eq.[3b] and Eq.[5b]. It has the advantage, that when the RF pulse amplitude is kept constant and the RF pulse duration is varied, (as done in Refs [5,6]) the optimum flip angle for short T2 tissues is always less than the classical Ernst angle. This makes the optimum flip angle more likely to be positioned in a regime where the underlying small tip angle approximation (and hence Eq.[3a]) is valid. Furthermore, since one can set B_1 to its maximum and then find the corresponding optimum τ, it takes only one iteration to find the best overall RF pulse.

Once the optimum pulse parameters are determined, the optimum flip angle in the presence of short T2 tissues (the generalized Ernst angle) can be calculated from the scaled RF profile using Eq.[1] in discrete form $\theta = \gamma \int_0^\tau B_1(t)dt = \gamma \Delta t \alpha \beta \sum_{n=1}^{N} B_1(n)$.

For example, for a hard RF pulse (as used in 3D UTE) the expression in Eq.[4] results in a optimum calculated flip angle of:

$$\theta \approx \sqrt{\frac{1 - E_1}{E_1 \left[\frac{T_2}{\tau} + \left(\frac{T_2}{\tau} \right)^2 \left(\exp\left(\frac{-\tau}{T_2} \right) - 1 \right) \right]}} \quad (6)$$

which for low flip angles can be shown to be a good approximation to the simulated results from Springer et al [4].

Methods

All experiments were conducted on a clinical 3T MR imaging system (Signa HDx, GE Medical Systems, Milwaukee, WI).

Phantoms

The phantom setup (shown in Fig. 3) consists of spherical phantoms filled with water doped with Gadolinium and $MnCl_2$ resulting in the measured T1's and T2's listed in Table 1. Coronal 2D UTE images were obtained using a standard transmit/receive (T/R) 8-channel knee coil with TE = 12 μs and TR = 50 ms, using a typical RF pulse (e.g. see Fig. 7a) of constant RF amplitude and variable pulse durations of $\tau \approx 0.5 – 5$ ms corresponding to flip angles of $\theta = 8 – 80°$.

In-vivo

Axial 2D UTE images of the lower leg of a 59-year old male volunteer were obtained to image the short T2 signal from the cortex of the tibia (T1 ≈ 200–300 ms, T2 ≈ 250–350 μs). Dual echo subtraction [10, 11] with TE1 = 12 μs and TE2 = 2.3 ms was used in order to suppress longer T2 tissue signals. Several images at nominal flip angles $\theta = 16 – 44°$ were obtained using a RF half pulse with constant RF duration $\tau = 970$ μs. Signal reception was achieved with a 3-inch surface coil.

Results

Theory

Fig. 4 shows theoretical optimum flip angles (lines) vs. T_2 for several values of TR/T_1 along with simulated results (markers) using a typical shaped RF pulse for 2D UTE imaging with N = 121. Fig. 4a shows the case for which the flip angle was varied by varying the RF amplitude (β) using a constant RF duration $\tau = 484$ μs ($\alpha = 4$), while Fig. 4b shows the case for which the flip angle was varied by varying the RF duration (α) using a constant RF amplitude of $B_1 = 15$ μT ($\beta = 15$).

As was also observed in [4], the optimum flip angles for Fig. 4a are always higher than the corresponding classical Ernst angles (horizontal lines), while the optimum flip angles for Fig. 4b are always lower ([5, 6]). In both cases the optimum flip angles converge to the classical Ernst angle in the limit where $T2 \rightarrow \infty$.

Phantoms

The signal intensities measured in small regions of interest (ROIs) at the center of each phantom (see Fig. 3) are shown in Fig. 5a as a function of flip angle. The corresponding theoretical signal intensities using Eq.[3a] (broken lines) and Bloch equation simulations (solid lines) are shown in Fig. 5b.

The classical and generalized Ernst angles as well as simulated and experimentally determined optimum flip angles are summarized in Table 1.

Several features can be observed from Fig. 5 and Table1: The simulated and experimental data agree reasonably well for all phantoms. The classical Ernst angle agrees with the simulated/experimental optimum flip angles for longer T2 phantoms (columns 1–3), but breaks down for the three shortest T2 phantoms (columns 4–6) as expected. Finally, the generalized Ernst angle agrees well for the three shortest T2 phantoms but there are deviations for the longer T2 phantoms as an expected consequence of operating outside the low flip angle approximation. In vivo tissues generally have longer T1s than the phantoms used here, which means that the optimum flip angles are typically lower so that the small flip angle approximation is more readily satisfied.

In-vivo

Fig. 6 shows the first echo, second echo, and subtraction of axial in-vivo 2D UTE scans of the cortex of the tibia. The top row shows the images obtained at the classical Ernst angle ($\theta \approx 23°$) for a typical RF half pulse (see Fig. 7a) with constant RF duration $\tau = 970$ μs, while the bottom row shows images obtained at the generalized Ernst angle ($\theta \approx 35°$) obtained from Eq.[4] and the RF waveform shown in Fig. 7a. The subtraction image obtained at the generalized Ernst angle exhibits similar SNR and contrast inside the cortical bone than the corresponding image obtained at the classical Ernst angle.

To assess the short T2 signal more quantitatively, the signal intensities measured in a small ROI within the cortical bone in the subtraction images is plotted as a function of θ in Fig. 7b. (Note: The ROI placement in Fig. 6 is shown in the second echo image in order not to obscure the cortical bone in the subtraction image). The maximum signal is reached at approximately $\theta \approx 36°$ (in good agreement with our theoretical prediction of $\theta \approx 34°$), and is about 13% higher than the signal obtained at the classical Ernst angle ($\theta \approx 23°$).

Discussion

We have derived an analytic expression for the steady state transverse magnetization resulting from VERSE corrected 2D UTE excitation RF pulses, and have used this to predict the optimum flip angles (generalized Ernst angles) for imaging of short T2 tissues. Simulations and experimental studies in phantoms and in-vivo support the validity of the

theoretical results. Practical considerations: Two methods for optimizing the nominal flip angle were presented. In method 1 the RF amplitude was optimized for a constant RF duration, while in method 2 the RF duration was optimized for a constant RF amplitude. While method 2 can potentially be used to obtain the overall best RF pulse using the highest available RF power, it is less flexible, since a new RF waveform would have to be created and loaded for different tissues. Method 1 is easier to implement on clinical scanners since for a given external RF pulse waveform, the flip angle is scaled via the RF amplitude, and so the same RF waveform can be re-used for applications in different tissues.

The results in this work were derived using the classical Bloch equations assuming irreversible T2 decay arising from homogeneous line broadening. Since T2 is hard to measure in musculoskeletal (MSK) tissues with rapid transverse relaxation times (e.g cortical bone), typically only T2* values are known, and these include contributions from T2' ($1/T2' = 1/T2^* - 1/T2$) decay arising from inhomogeneously broadened lines. While the two different mechanisms by themselves result in identical free induction decay behavior and hence T2*, they do not follow exactly the same magnetization trajectory during the application of RF pulses [12]. Since in vivo tissues usually have contributions from both homogeneously and inhomogeneously broadened lines, inclusion of these in a more complex model may slightly alter the derived optimum flip angle optimization. While this effect is small when $TR \ll T1$, this may play an important part in tissues containing high susceptibility background fields such as imaging around metal implants. Further investigations may be necessary to assess the impact of this on our results.

References

1. Gatehouse PD, Bydder GM. Magnetic resonance imaging of short T2 components in tissue. Clin Radiol. 2003; 58:1–19. [PubMed: 12565203]
2. Tyler DJ, Robson MD, Henkelman RM, Young IR, Bydder GM. Magnetic resonance imaging with ultrashort TE (UTE) PULSE sequences: technical considerations. J Magn Reson Imaging. 2007; 25(2):279–89. [PubMed: 17260388]
3. Robson MD, Gatehouse PD. Consequences of T2 Relaxation During Half-Pulse Slice Selection for Ultrashort TE Imaging. Magn Reson Med. 2010; 64:610–615. [PubMed: 20665804]
4. Springer F, Steidle G, Martirosian P, Claussen CD, Schick F. Effects of in-pulse transverse relaxation in 3D ultrashort echo time sequences: Analytical derivation, comparison to numerical simulation and experimental application at 3T. J Magn Reson. 2010; 206:88–96. [PubMed: 20637661]
5. Carl M, Bydder M, Du J, Takahashi A, Han E. Optimization of RF Excitation to Maximize Signal and T2 Contrast of Tissues With Rapid Transverse Relaxation. Magn Reson Med. 2010; 64:481–490. [PubMed: 20665792]
6. Carl, M.; Bydder, M.; Takahashi, A.; Han, E.; Bydder, G. Maximizing RF Signal in the Presence of Rapid T2 Relaxation. Proceedings of the 17th Annual Meeting of ISMRM; 2009; Honolulu, Hawaii, USA. p. 1991
7. Nishimura, DG. Principles of Magnetic Resonance Imaging. 1.1. Stanford University Press; Palo Alto: 2010. Published by
8. Hargreaves BA, Cunningham CH, Nishimura DG, Conolly SM. Variable-Rate Selective Excitation for Rapid MRI Sequences. Magn Reson Med. 2004; 52:590–597. [PubMed: 15334579]
9. Bernstein, MA.; King, KF.; Zhou, XJ. Handbook of MRI Pulse Sequences. Elsevier Academic Press; London: 2004.

10. Rahmer J, Blume U, Bornert P. Selective 3D ultrashort TE imaging: comparison of “dual-echo” acquisition and magnetization preparation for improving short-T2 contrast. MAGMA. 2007; 20(2): 83–92. [PubMed: 17354002]

11. Robson MD, Benjamin M, Gishen P, Bydder GM. Magnetic resonance imaging of the Achilles tendon using ultrashort TE (UTE) pulse sequences. Clin Radiol. 2004; 59(8):727–35. [PubMed: 15262548]

12. Carl, M.; Szeverenyi, N.; Bydder, M.; Han, E.; Bydder, G. MR Spin Behavior During RF Pulses: T2 vs T2′ Relaxation. Proceedings of the 18th Annual Meeting of ISMRM; 2010; Stockholm, Sweden. p. 800

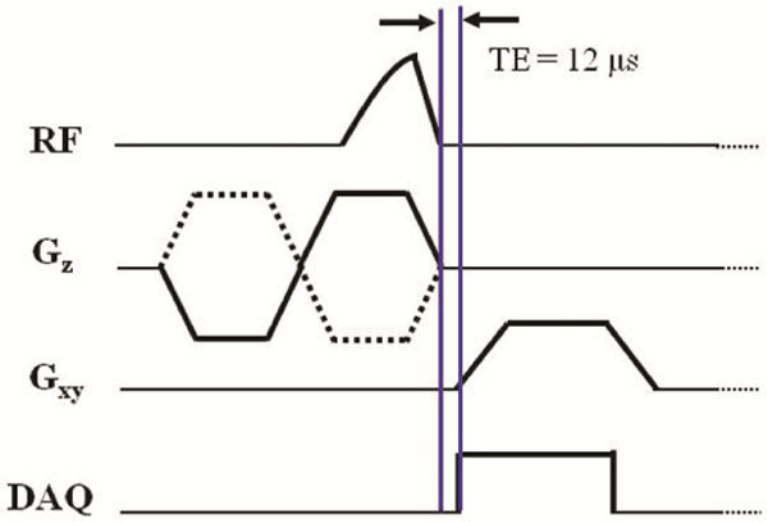

Fig. 1.

Schematic diagram of a 2D UTE sequence of nominal TE = 12 μs (arrows). The last part of the RF pulse is applied during the ramp-down portion of the slice selective gradient G_z. Data acquisition (DAQ) is started during the ramp-up portion of the read gradients G_x and G_y.

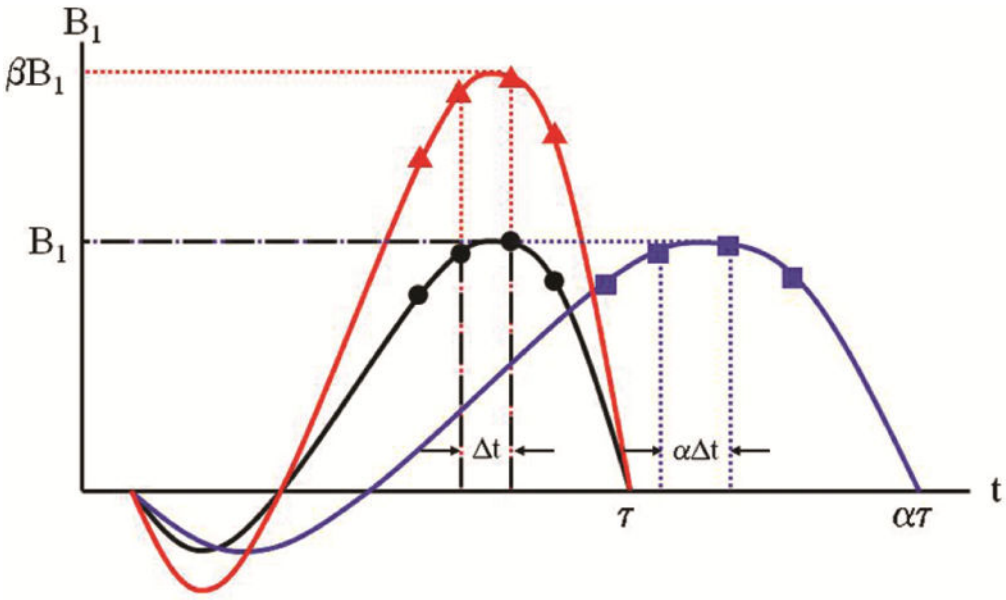

Fig. 2.

RF pulse shape. The original waveform is shown in black. The spacing Δt of the discrete RF waveform points (black circles) is shown but is exaggerated along the time axis (t) for clarity. A typical 800 μs RF pulse with 4 μs RF raster time for example would contain N = 200 points. In order to increase the flip angle, the waveform may be time-stretched (blue squares), or amplitude-stretched (red triangles).

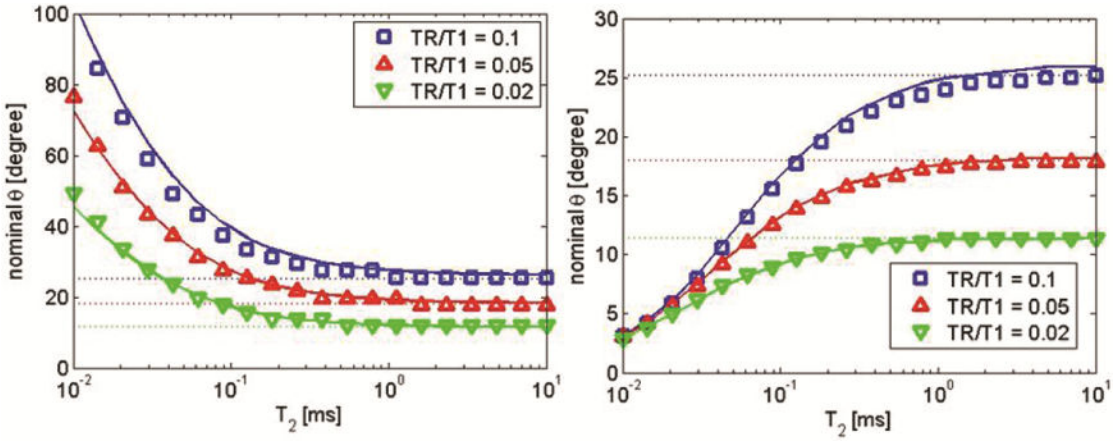

Fig. 3.

2D UTE image of a phantom consisting of plastic spheres filled with water doped with Gadolinium and $MnCl_2$ resulting in the measured T1 and T2 parameters listed in Table 1. The mean signals within the colored ROIs are plotted in Fig. 5.

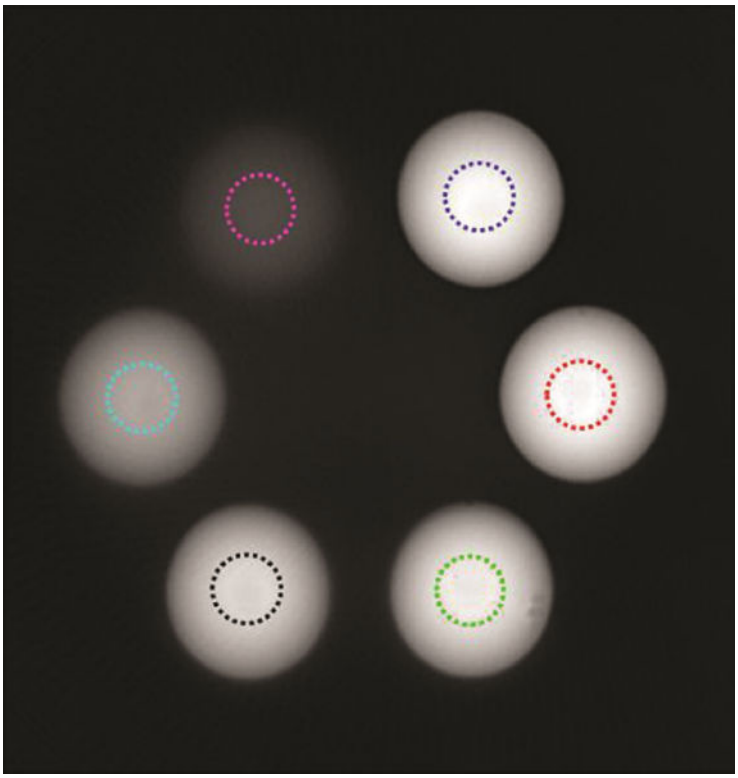

Fig. 4.

Optimum nominal flip angle vs. T_2 case with a constant using a N = 121 shaped RF pulse. Part a) shows the τ, and variable B_1. The optimum flip angle is always higher than the classical Ernst angle (horizontal lines) in agreement with [4]. Part b) shows the case for constant B_1, and variable τ. The optimum flip angle is always lower than the classical Ernst angle in agreement with [5, 6].

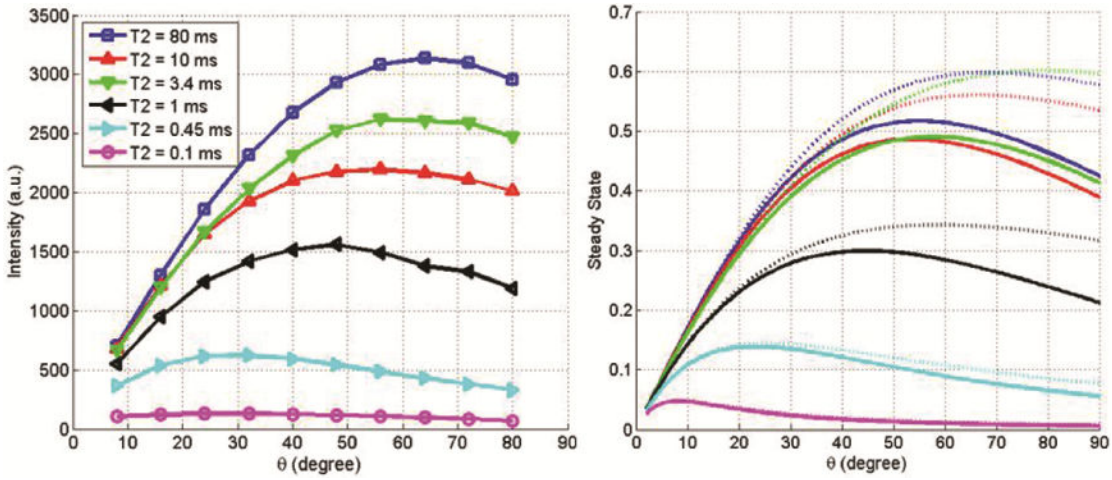

Fig. 5.

a: Experimental signal intensities (const B_1). b: Simulated (solid) and theoretical (dashed) signal intensities (const B_1). The generalized Ernst angle agrees well for the three shortest T2 phantoms but there are deviations for the longer T2 phantoms as an expected consequence of operating outside the low flip angle approximation.

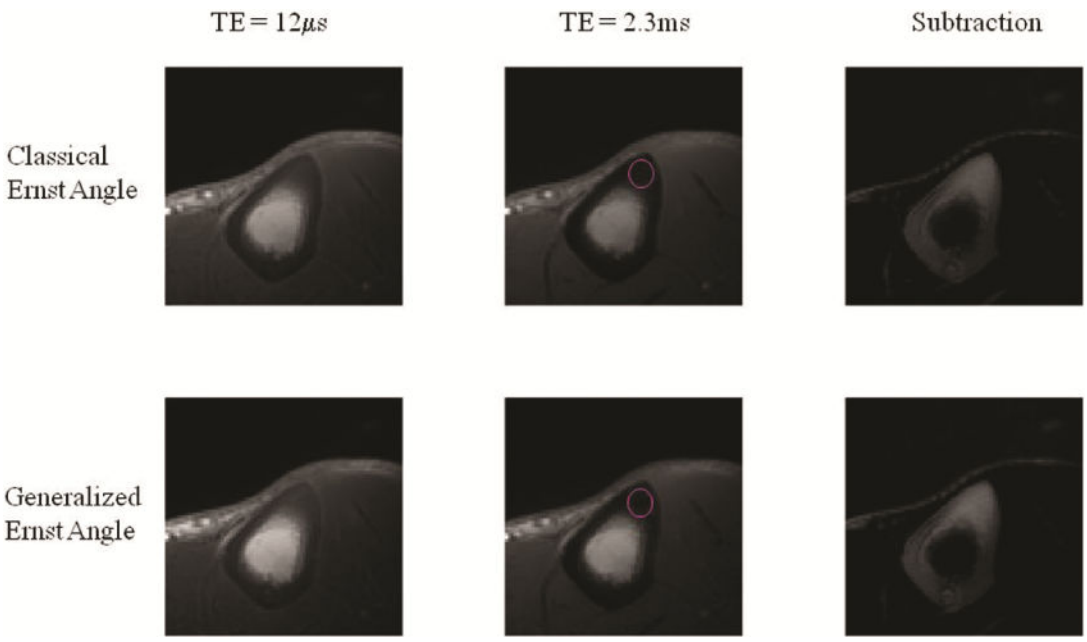

Fig. 6.

In vivo 2D UTE images of the cortex of the tibia. The top row shows images obtained at the classical Ernst angle ($\theta \approx 23°$) for a constant RF duration $\tau = 970$ μs, while the bottom row shows images obtained at the generalized Ernst angle ($\theta \approx 34°$) obtained using Eq.[4]. The ROI placement inside the cortical bone is shown in the second echo in order not to obscure the cortical bone in the subtraction image, however the signal levels from cortical bone that are plotted in Fig. 7b as a function of θ were measured on the subtraction image.

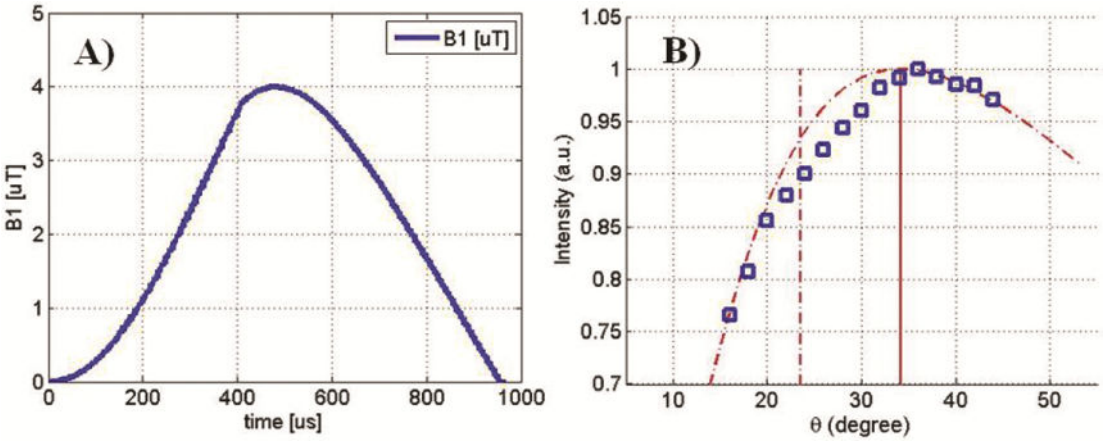

Fig. 7.

A) 2D UTE (VERSE corrected) RF pulse shape used in the in-vivo experiments shown in Fig. 6. B) Signal intensities for cortical bone are shown as a function of θ. Note that the maximum signal is reached at approximately $\theta \approx 36°$, in good agreement with the theoretical prediction (red dashed curve) of $\theta \approx 34°$ (solid vertical line). The experimental signal at $\theta \approx 36°$ is about 13% higher than the signal at the classical Ernst angle at $\theta \approx 23°$ (dashed vertical line).

Table 1

Approximate classical and generalized Ernst angles as well as simulated and experimental optimum flip angles for the phantom data shown in Fig. 5. The generalized Ernst angle agrees well for the three shortest T2 phantoms but there are deviations for the longer T2 phantoms as an expected consequence of operating outside the low flip angle approximation.

	T1 ≈ 90 [ms] T2 ≈ 80 [ms]	**T1 ≈ 85 [ms] T2 ≈ 10 [ms]**	**T1 ≈ 49 [ms] T2 ≈ 3.4 [ms]**	**T1 ≈ 20 [ms] T2 ≈ 1.0 [ms]**	**T1 ≈ 15 [ms] T2 ≈ 0.45 [ms]**	**T1 ≈ 10 [ms] T2 ≈ 0.1 [ms]**
Classical Ernst	56°	56°	69°	85°	88°	90°
General Ernst	69°	67°	79°	58°	25°	8°
Sim. Theta	56°	53°	58°	47°	23°	8°
Exper. Theta	62°	55°	65°	48°	27°	SNR too low